Cancer Cell International

RESEARCH

Open Access

The genomic landscape of esophageal squamous cell carcinoma cell lines

Chao Zhang[1,2,3†], Chenghao Li[4†], Jian Zhong Su[5], Kuaile Zhao[3,6,7,8], Longlong Shao[1,2,3*] and Jiaying Deng[3,6,7,8*]

Abstract

Background Research on the genomic characteristics of common esophageal squamous cell carcinoma (ESCC) cell lines, including exome mutations and mRNA expression, is limited. This study aims to elucidate the malignancy, invasion capability, classical cancer-related signaling pathways, and immune status of ESCC cell lines, providing a detailed genomic landscape and highlighting the unique features of each cell line.

Methods Whole exome and RNA sequencing were conducted on ESCC cell lines TE-1, ECA-109, KYSE-30, KYSE-150, KYSE-180, KYSE-450, and KYSE-510, with the normal epithelium cell line Het-1a as a comparison. Bioinformatics methods analyzed gene mutation types, mutation frequencies, RNA expression, and classical cancer-related signaling pathways. Specific analyses were also performed on tumor burden, genes related to differentiation, invasion, immunity, and gene enrichment in each cell line.

Results The highest tumor mutation burden (TMB) was 70.4 mutations per megabase (mut/MB) in KYSE-150, while the lowest was 48.7 mut/MB in KYSE-510. Mutations in the Hippo, Notch, PI3K, RTK-Ras, and Wnt signaling pathways were present in all cancer cell lines. Mutations were significantly enriched in signature 3, associated with defective homologous recombination deficiency (HRD). The NRF2 signaling pathway exhibited mutations in KYSE-180, KYSE-450, and TE-1 cell lines. The cell cycle gene mutation frequency was low, occurring only in KYSE-30 and TE-1 cell lines. The expression profiles of KYSE-510 and ECA-109 were similar. The KYSE-150 cell line showed up-regulated invasion genes, while the KYSE-450 cell line had significantly down-regulated poor differentiation-related genes. Immune-related genes were up-regulated in the ECA-109 cell line.

Conclusion The molecular profiles generated in this study provide detailed information on gene mutations and expression in common ESCC cell lines. The KYSE-150 cell line exhibited a prominent invasion capability, while the ECA-109 cell line showed up-regulated immune properties. This genomic landscape offers valuable insights for future research and therapeutic strategies in ESCC.

†Chao Zhang and Chenghao Li contributed equally to this work.

*Correspondence:
Longlong Shao
shaollong@163.com
Jiaying Deng
dengjiaying3@sina.com
[1]Departments of Thoracic Surgery, State Key Laboratory of Genetic Engineering, Fudan University Shanghai Cancer Center, Shanghai 200032, China
[2]Institute of Thoracic Oncology, Fudan University, Shanghai 200032, China
[3]Department of Oncology, Shanghai Medical College, Fudan University, Shanghai 200032, China
[4]School of Life Science and Technology, State Key Laboratory of Urban Water Resource and Environment, Harbin Institute of Technology, Harbin 150006, Heilongjiang, China
[5]School of Biomedical Engineering, School of Ophthalmology and Optometry and Eye Hospital, Wenzhou Medical University, Wenzhou 325011, China
[6]Department of Radiation Oncology, Fudan University Shanghai Cancer Center, Shanghai 200032, China
[7]Shanghai Clinical Research Center for Radiation Oncology, Shanghai 200032, China
[8]Shanghai Key Laboratory of Radiation Oncology, Shanghai 200032, China

Introduction

Esophageal squamous cell carcinoma (ESCC) is the sixth most common cancer worldwide [1]. It arises due to a variety of etiologic factors, including tobacco exposure, alcohol consumption, and vitamin deficiency. Metastasis is the significant failure pattern after neoadjuvant chemoradiotherapy in ESCC, as highlighted by the CROSS and NEOCRTEC5010 studies [2, 3]. The Cancer Genome Atlas and other genomic sequencing studies have begun to characterize the mutational landscape of ESCC [4, 5]. One key finding is that NFE2L2 (NRF2) mutation is a race-specific genomic feature, differentiating between Asian and Caucasian ESCC populations [6]. This mutation has led to the definition of an NFE2L2-mutated subtype as one of three ESCC subtypes [7]. Consequently, targeted therapeutic drugs based on NFE2L2 mutations in ESCC are gaining more attention.

Despite these advancements, there is still a need for follow-up in vitro studies to investigate vital regulatory pathways, confirm malignant drivers, and identify potential therapeutic targets in genetically characterized models. Keynote studies on the immunotherapy of ESCC have indicated that esophageal cancer has relatively strong immunogenicity [8, 9]. Research has correlated immune-related genes in ESCC tumor tissue with prognosis [10]. However, there is limited research on the mutation status and expression of immune-related genes in ESCC cell lines. Additionally, the differentiation or malignant degree of common ESCC cell lines still requires further investigation.

Given the potential for wide phenotypic variations based on genetic mutations and the move towards genetics-based personalized medicine approaches, understanding the genetic architecture of cell lines used for in vitro studies is increasingly essential. However, the full genetic characterization of ESCC cell lines has not yet been performed.

In this study, we sought to catalog several ESCC cell lines' mutational landscapes and identify critical metastasis, differentiation, and immunogenicity genes. By indicating the background status and expression of critical pathways, including the cell cycle, NRF2, Notch, Wnt, Epigenetic, and PI3K pathways, we aim to provide a foundation for future in vitro research.

Methods

Cell lines

The normal esophageal epithelium cell line Het-1a and ESCC cell lines (TE-1, ECA-109, KYSE-30, KYSE-150, KYSE-180, KYSE-450, and KYSE-510) were obtained from the Shanghai Institute for Biological Sciences, Chinese Academy of Sciences. All cell lines were identified with Short Tandem Repeat (STR) profiling by the Shanghai BIOWING company. Cells were cultured in RPMI-1640 or DMEM media, supplemented with 10% fetal bovine serum (FBS), ampicillin (50 U/ml), and streptomycin (50 μg/ml), in a humidified incubator at 37°C with 5% CO2.

Exome sequencing

Whole genomic DNA was isolated using the Qiagen DNeasy Blood & Tissue kit according to the manufacturer's instructions. Exome Capture Library Construction was performed using the Roche NimbleGen V3. Paired-end sequencing (2 × 150 bp) of the captured exons was conducted using the Agilent SureSelect All Human Exome library_60M (V6).

RNA sequencing

RNA was isolated with a TRIzol reagent. Libraries were prepared according to the manufacturer's protocols using the Illumina Total RNA kit. Read quality was assessed using FastQC (v0.11.5). Read alignment was performed using STAR (v2.5.3a) following the two-step alignment protocol recommended in the user manual. Cufflinks (v2.2.1) were used to compute Fragments Per Kilobase of transcript per Million mapped reads (FPKM), and values were loaded into MEV to visualize relative expression.

FPKM normalizes gene expression levels by factoring in gene length and the total number of mapped reads per sample. However, the sum of all mapped reads in a sample are first divided by a million to obtain a per million scaling factor for the sample. This per sample scaling factor is then used to scale the mapped reads of every gene. The scaled gene data is eventually normalized by dividing each gene by its corresponding gene length (in kB), thus, obtaining FPKM.

Bioinformatic analysis

Read quality was assessed using FastQC v.0.11.9. Reads were aligned to the hg19 reference genome using BWA v0.7.8 [11]. PicardTools v1.79 (Broad Institute) was used to mark duplicates and conduct the mapping. INDEL realignment was performed using GATK v3.2-2 [12]. Variant calling was conducted using the HaplotypeCaller available on the GATK4 website to produce a Variant Call Format (VCF) file for each sample. VCFs were combined using Genotype GVCFs across all samples [13].

Data alignment and quality control

Whole exome sequencing (WES) data were processed following standard bioinformatics pipelines. Raw paired-end FASTQ files were trimmed and adapter sequences removed using Cutadapt. The cleaned reads were then aligned to the human reference genome (Homo sapiens assembly 38) using BWA MEM (version 0.7.17), with the -M flag applied to mark duplicate reads and incorporating relevant read group information. The generated SAM

file was subsequently converted into BAM format using samtools view. The BAM file was then sorted by genomic coordinates with samtools sort, followed by removal of duplicate reads using Picard's MarkDuplicates tool, yielding a high-quality deduplicated BAM file for downstream analysis.

Base quality score recalibration and variant calling

To enhance the accuracy of variant calling, base quality score recalibration (BQSR) was performed using the GATK BaseRecalibrator tool, leveraging known SNP and indel databases, including dbSNP, Mills, and 1000G gold standard. The recalibration table was then applied to the deduplicated BAM file with ApplyBQSR, producing a corrected BAM file for subsequent variant calling. Somatic variant detection was carried out using GATK's Mutect2, generating a VCF file containing high-confidence mutations identified across the exome.

Mutation filtering

Subsequent to variant calling, stringent quality control measures were applied to filter out potential false-positive calls and retain only those mutations with high confidence. Variants with a quality by depth (QD) score below 4.0 were excluded, as they typically represent low-confidence calls due to inadequate sequencing depth. Mutations with a quality score (QUAL) below 40.0 were similarly discarded to maintain high data integrity. Variants exhibiting a strand odds ratio (SOR) greater than 6.0, which suggests strand bias, were filtered out, along with those with a Fisher strand (FS) score exceeding 120.0, indicative of potential sequencing artifacts. Variants with a mapping quality (MQ) score below 40.0 were removed to exclude those with suboptimal alignment, while mutations with a mapping quality rank sum (MQRankSum) score lower than − 12.5 were also excluded, as these suggest potential misalignments. Finally, variants exhibiting a read position rank sum (ReadPosRankSum) score lower than − 16.0 were filtered to remove those with atypical read distributions. This comprehensive filtering strategy ensured that only high-confidence somatic mutations, free of technical biases and sequencing errors, were retained for downstream analysis. MutSigCV was applied to identify significantly mutated genes with default covariate tables. Genes with q (FDR) < 0.1 were considered to be significantly mutated.

The Affymetrix OncoScan Assay kit was used to analyze copy number alterations in these cell lines. CEL files from the kit were combined to produce OSCHP files using the OncoScan Console v1.3 software. These OSCHP files were analyzed using the TuScan algorithm of the Nexus Express for OncoScan Software.

Results

Mutational signatures of ESCC Cell lines

SMGs

The mean sequencing coverage for whole-exome sequencing (WES) was 100× for these cell lines. 74,848 somatic mutations were detected, including single nucleotide variants (SNVs) and small insertions and deletions (InDels). Detailed sequencing data are provided in supplementary Table 1. Tumor mutational burden (TMB), an effective biomarker for immunotherapy, was calculated for these cell lines. The highest TMB was observed in KYSE-150 (70.4 mutations per megabase), and the lowest was in KYSE-510 (48.7 mutations per megabase). Other TMB values ranged between 49.9 and 64.8 (Fig. 1-A).

The MutSigCV method was used to identify significant mutation genes (SMGs) in the combined seven ESCC cell lines (Fig. 1-A). Genes with a 100% mutation frequency included ZFHX4, PKHD1, ABCA13, OBSCN, IGFN1, PCLO, MUC16, and TTN. The ZFHX4 indel mutation was unique to the KYSE-510 cell line. High-frequency missense mutations were found in various genes across different cell lines, such as CSMD3, TP53, PLEC, NOTCH2, EYS, FAT2, NOTCH1, and NOTCH3 in KYSE-150; ZFHX4, CSMD3, EYS, FAT2, FAT1, FAT4, and CSMD1 in KYSE-450; and CSMD3, EYS, FAT2, COL6A5, and BRCA2 in KYSE-510. The results of MutSigCV was showed in the supplementary Table 2.

Mutations signature

To understand the contribution of these mutations to ESCC etiology, mutational signatures were analyzed using the COSMIC (Catalogue of Somatic Mutations in Cancer) database. Mutations in each cell line were enriched in signature 3, associated with defective homologous recombination deficiency (HRD) (Fig. 1-B).

HRD genes

We performed RNA-seq for these cell lines and provided all data in supplementary Table 3. Based on the FPKM value, the relative mRNA expression of HRD genes in ESCC cell lines was significantly higher than in normal epithelial cell (Het-1 A; Fig. 1-C). Expression of HRD genes with wild-type alleles was significantly higher than mutated HRD genes in ESCC cell lines (Fig. 1-D). The HRD panel included 18 genes, such as BRCA1, BRCA2, CHEK2, FANCE, and MSH2, detailed in the supplementary Table 4. A deleterious germline mutation BRCA1: p.Leu52Phe was found in the TE-1 cell line.

Gene mutation in classical cancer-related signaling pathways

Sequencing studies indicated that classical signaling pathways are dysregulated in ESCC via genomic and epigenomic aberrations. NRF2 (encoded by NFE2L2)

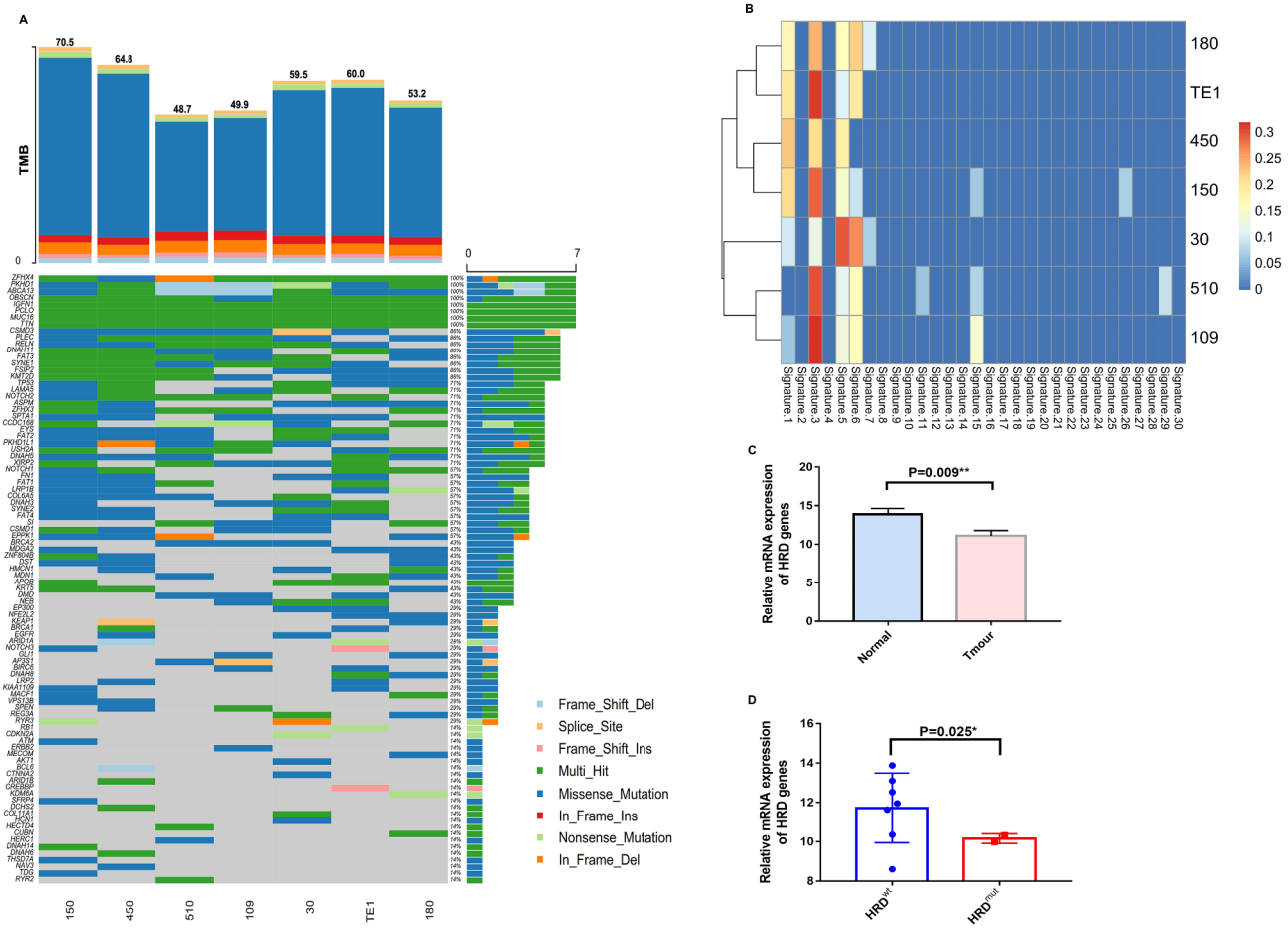

Fig. 1 **A**. Tumor mutation burden (TMB) and significant mutated genes identified by MutSigCV and OncodriveFML with q value < 0.1 in ESCC cell lines. Rows are genes and columns are cell lines. The TMB is shown in the upper panel. **(B)** Gene enrichment according to COSMIC database. **(C)** The expression of homologous recombination deficiency(HRD)genes between normal epithelial cell and cancer cell lines. **(D)** The expression of homologous recombination deficiency (HRD) genes between wild type and mutation

activates transcription of genes that control oxidative stress, while KEAP1 interacts with CUL3 to target NRF2 for degradation through the ubiquitin-proteasome system.

A Go pathway analysis was conducted to understand the mutation status of classical cancer signaling pathways. Results showed that genes in the Hippo, NOTCH, PI3K, RTK-Ras, and Wnt signaling pathways were mutated in TE-1, ECA-109, KYSE-30, KYSE-150, KYSE-180, KYSE-450, and KYSE-510 cell line (Fig. 2-A). The mutation rate of the NRF2 signaling pathway was 42.9%, with mutations in KEAP1, NRF2, and CUL3 present only in KYSE-180, KYSE-450, and TE-1 cell lines (Fig. 2-B). The cell cycle signaling pathway had a relatively low mutation rate of 28.6%, with mutations in CDKN2A and RB1 occurring only in KYSE-30 and TE-1 cell lines. No mutations in the TP53 signaling pathway were found in KYSE-510 and ECA-109 cell lines, and no mutations in the TGF-β pathway were found in KYSE-510, KYSE-30, and ECA-109 cell lines (Fig. 2-B).

Copy number variation (CNV) in classical cancer-related signaling pathways

Chromosome CNV profiling revealed chromosome 13 amplification in these cell lines. The focal amplifications and deletions are shown in Supplementary Fig. 1. We analyzed CNV in classical cancer-related signaling pathways in each cell line (Fig. 2-C).

In the TE-1 cell line, copy number loss frequently occurred in the focal cell cycle, RTK, and Wnt signaling pathways. The KYSE-30 cell line, copy number amplification of the MYC and NOTCH signaling pathways was observed. In the KYSE-150 cell line, copy number loss of the cell cycle and Hippo signaling pathways and copy number amplification of TGF-β were observed. The CNV landscape of the ECA-109 and KYSE-510 was similar, with copy number amplification of Hippo, Notch, PI3K, TGF-β, and Wnt signaling pathways in both cell lines. In the KYSE-180 cell line, copy number loss frequently occurred in the focal cell cycle, Hippo, genes including

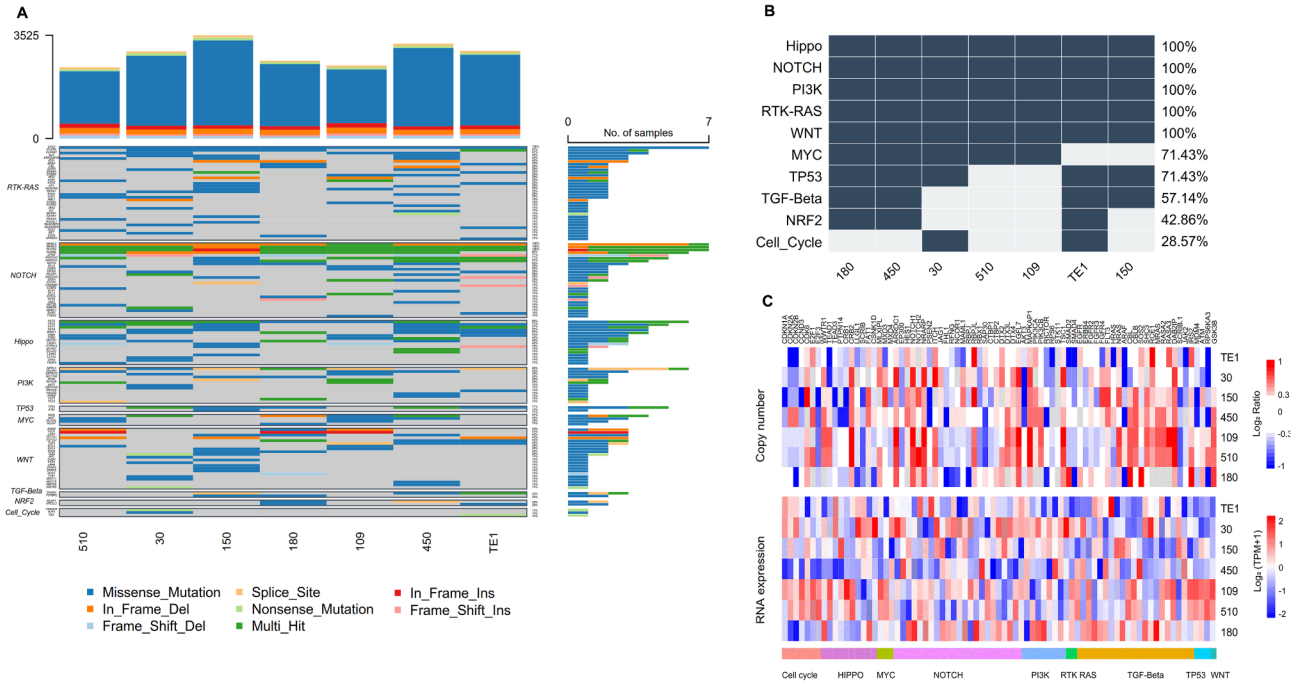

Fig. 2 **(A)** Gene mutation of classical cancer-related signaling pathways in ESCC cell lines. **(B)** Mutation frequency of classical cancer-related signaling pathways in ESCC cell lines. **(C)** Copy number variations (CNV) and RNA expression of classical cancer-related signaling pathways in ESCC cell lines

FHL1, RFNG, NCOR1 for Notch, RICTOR for PI3K, and ARAF for TGF-β signaling pathways.

The expression of key genes in classical cancer-related signaling pathways

We also performed RNAseq for these cell lines and provided all data in supplementary Table 3. In all comparisons, the expression of genes in Her-1 A was the reference standard. We analyzed gene expression in the cell cycle, Hippo, MYC, NOTCH, PI3K, RTK-RAS, TGF-β, TP53, and Wnt signaling pathways (Fig. 2-C). In the TE-1 cell line, HRAS for TGF-β was significantly up-regulated. In the KYSE-30 cell line, LLGL1 and CSNK1D for Hippo, ARRDC1 for Notch, TSC1 for PI3K, and RCE1 for TGF-β were significantly up-regulated. These signaling pathways were relatively down-regulated in the KYSE-150 cell line. RBX1 for NOTCH and CBLB for TGF-β were significantly up-regulated in the KYSE-450 cell line. The expression landscape of KYSE-510 and EC-109 was similar: genes for the cell cycle, Hippo, TP53, and Wnt signaling pathways were up-regulated. In the KYSE-180 cell line, NOTCH, PI3K, and TGF-β signaling pathways were relatively up-regulated.

The clustering heatmap of classical cancer-related signaling pathways

To compare CNV and gene expression in classical cancer-related signaling pathways, the clustering heatmap was conducted and showed in Fig. 3. The results showed that the CNV distribution of ECA-109 and KYSE-510 cell lines was relatively uniform (Fig. 3A). PI3K, Hippo and Notch signaling pathways were copy number amplified in ECA-109 and KYSE-510 cell lines. CNV deletions of TP53, Hippo and Notch signaling pathways were showed in KYSE-450 and KYSE-150 cell lines. Gene expression distribution of classical cancer-related signaling pathways was showed in Fig. 3B. Diversity of distribution including over-expression and down-expression of signaling pathways were observed in each cell line. The expression landscape of KYSE-510 and ECA-109 were more similar than other cell lines.

Comparison of our analyzed results with CCLE data

There are almost 38 ESCC cell lines data in the Cancer Cell Line Encyclopedia (CCLE). Due to limitations in sequencing platforms and sequencing depth, we cannot directly combine our data with public CCLE data to analyze. But we analyzed the CCLE data again and observed the consistence between our results and CCLE data (Fig. 4). We can see that classical cancer-related signaling pathways including TP53, RTK-RAS, Notch, Hippo, Wnt and cell cycle pathways are all significantly enrichment both in our sequenced cell line and CCLE cell lines. Detailed gene mutation frequency and type for CCLE cell lines were showed in supplementary Fig. 2.

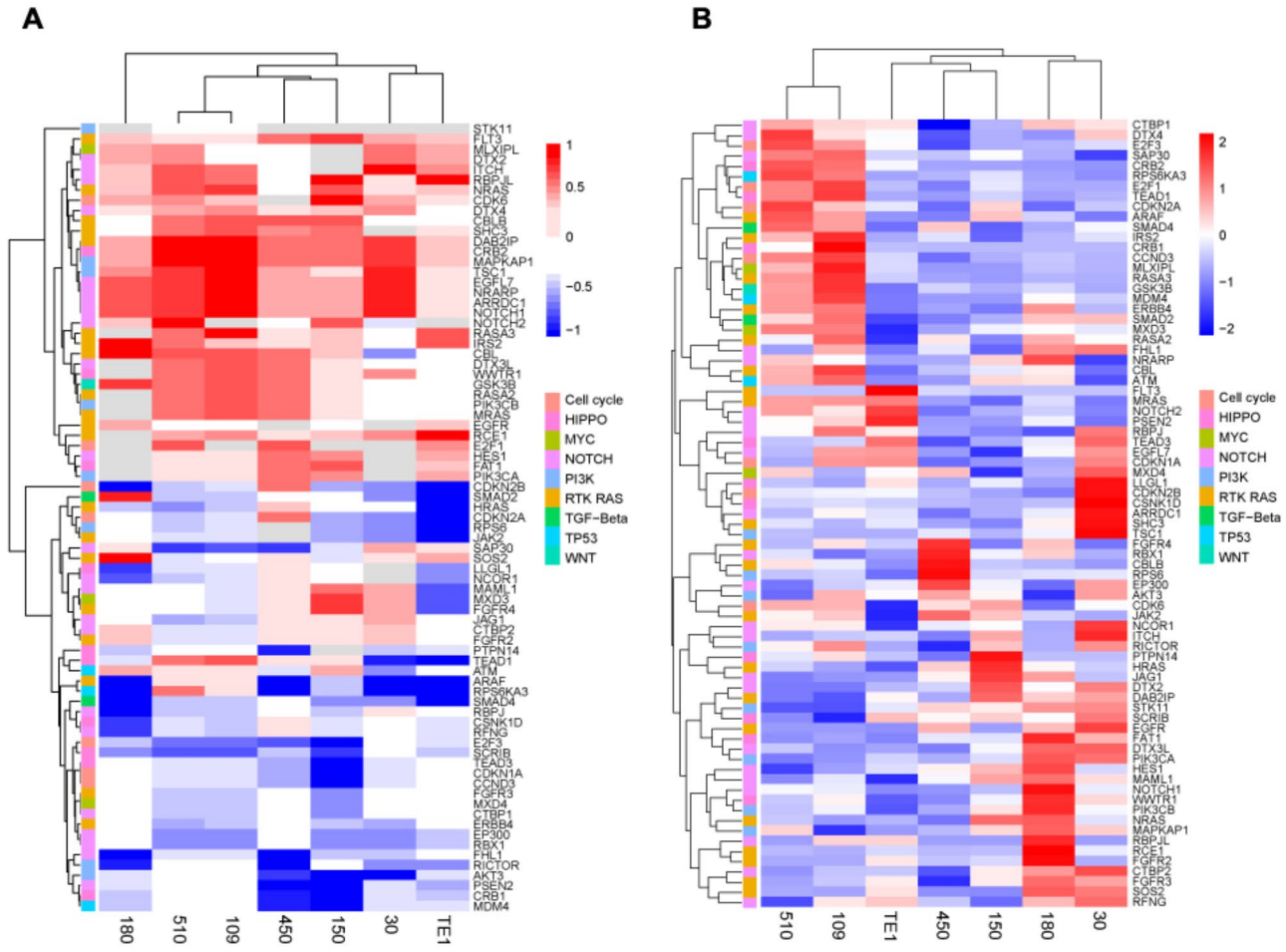

Fig. 3 **A.**The clustering heatmap of CNV in classical cancer-related signaling pathways. **B.** The clustering heatmap of gene expression in classical cancer-related signaling pathways

The expression of oncogenic related genes

We analyzed several oncogenic-related genes, including the NRF2 signaling pathway, Wnt signaling pathway, and invasion, differentiation, and immune-related genes based on published research (Fig. 5-A). The panel, including AREG, EREG, MMP1, IL6, MMP3, IL1B, and ADM, was chosen as markers for tumor invasion ability. Up-regulated invasion genes and Wnt signaling pathways were observed in the KYSE-150 cell line. Down-regulated invasion genes were observed in the KYSE-510, KYSE-180, and ECA-109 cell lines, suggesting that KYSE-150 might be the most malignant cell line (Fig. 5-B). Up-regulated and down-regulated NRF2 signaling pathways occurred in the KYSE-30 and ECA-109 cell lines, respectively (Fig. 5-C).

An integrated analysis of well-differentiation-related genes, including EGFR, MET, CSK, and poor differentiation-related genes, including CCND1, CDKN1B, HSPBP1, CEACAM1, EPHA2, and CTNNA1, was also conducted in these cell lines. Poor differentiation-related genes were significantly down-regulated in the KYSE-450 cell line and up-regulated in the KYSE-30 and TE-1 cell lines (Fig. 5-D).

Regarding immune-associated genes such as F2R, CD40, IL3RA, and CXCR4, down-regulation of these genes occurred in the KYSE-30 and KYSE-450 cell lines. Immune-related genes were up-regulated in the ECA-109 cell line. Significant up-regulation of CD40 was observed in the TE-1 cell line (Fig. 5-E). Studies showed that up-regulation of these four genes was associated with poor prognosis. The appropriate cell line can be selected for the corresponding experiment according to the background immune status.

Discussion

Large-scale, sequenced analyses using tumor tissue have recently provided unparalleled genomic details toward ESCC, paving the way for precision medicine based on comprehensive molecular profiles [4, 5]. As to esophageal cell lines, previous research dates to 1984, focusing on the degree of keratinization and amino acid metabolism [14]. And studies have started characterizing the

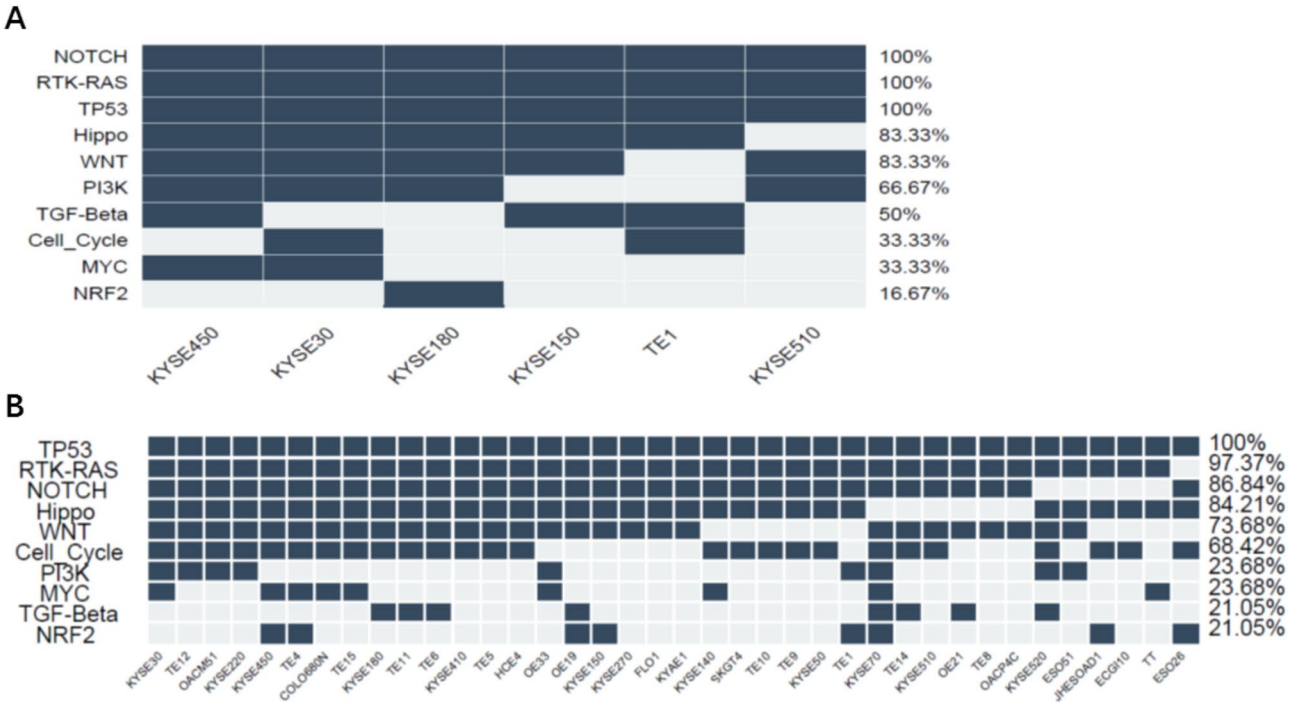

Fig. 4 **A.**Enrichment of classical cancer-related signaling pathways in the current analysis. **B.** Enrichment of classical cancer-related signaling pathways based on the CCLE data

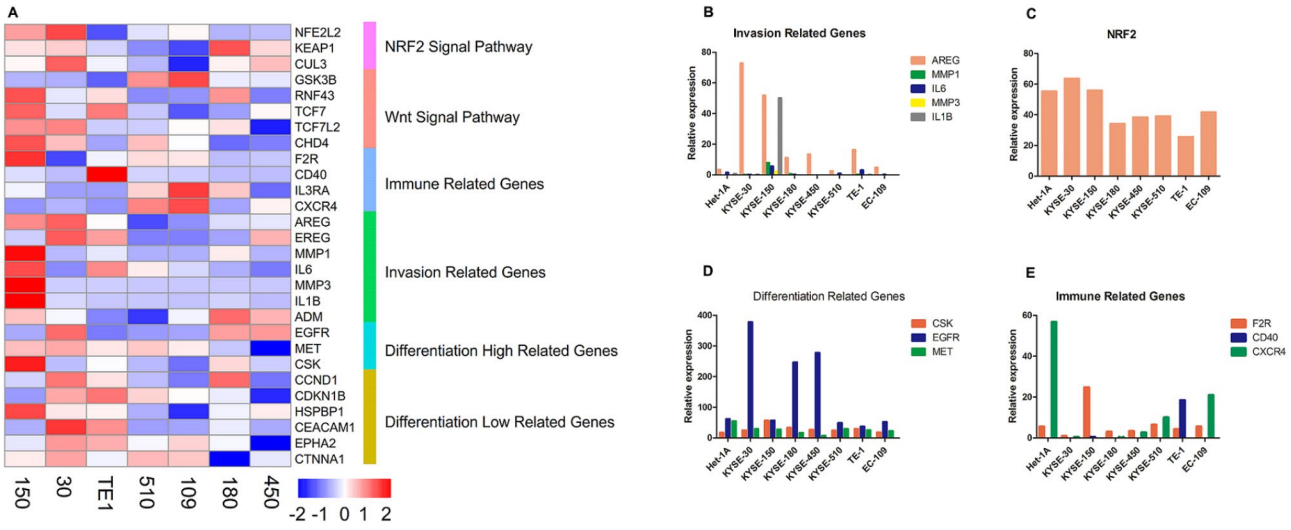

Fig. 5 **(A)** The expression of oncogenic related genes in ESCC cell lines. **(B)** Expression of invasion related genes expression in ESCC cell lines. **(C)** NRF2 expression in ESCC cell lines. **(D)** Expression of differentiation related genes in ESCC cell lines. **(E)** Expression of immune related genes in ESCC cell lines

genetic implications of therapeutic response in other cell line models, but this analysis has been limited in ESCC [15–17].

Genomic studies based on tumor specimens identified the NRF2 signaling pathway as a potential subtype of ESCC [7]. The current analysis showed that no mutation of NRF2 signaling pathway genes occurred in the KYSE-30, KYSE-510, KYSE-150, and EC-109 cell lines. Previous study showed that activation of NRF2 promotes radiochemoresistance in ESCC and lung cancer [18, 19]. Our unpublished data in ESCC also identified the conclusion. NRF2 inhibitor including small-molecule inhibitor (R16), Brusatol, ML385 and other developed chemical drug have been investigated in cancer therapy enhanced chemotherapeutic effects through inhibition of Nrf2/GPX4 signaling pathway or P62/Keap1/Nrf2 pathway [20–22]. Inhibition of NRF2 was promising in ESCC therapy and the Clinical trials website showed that a

series of NRF2 inhibitor are ongoing including I and II phase study. A First-in-Human (FIH) study to evaluate the safety and tolerability of VVD-130,037 in articipants with advanced solid tumors (NCT05954312) is recruiting. VVD-130,037 played as a Kelch-like ECH Associated Protein 1 (KEAP1) activator. KEAP1-NRF2 pathway activation promotes esophageal cancer cell proliferation and migration.

Based on cDNA microarray results, significant up-regulation of MET, EGFR, and CSK was correlated with high differentiation in ESCC, while up-regulation of CCND1, EPHA2, CEACAM1, HSPBP1, and CTNNA1 was associated with poor differentiation. Genomic studies also showed that up-regulation of MET is associated with high differentiation in ESCC [13]. Analysis of protein expression between esophageal cancer and dysplasia showed that CDKN1B was associated with the pathological degree and prognosis in ESCC [23].

Regarding immune-related genes, CD40 is a cell-surface member of the TNF (tumor necrosis factor) receptor. Upon activation, CD40 can license dendritic cells to promote antitumor T cell activation and re-educate macrophages to destroy tumor stroma. Immunological research showed that combinatorial immunotherapy with agonistic CD40 activates dendritic cells to express IL12 and overcomes PD-1 resistance [24]. Numerous agonist CD40 antibodies of varying formulations have been evaluated in clinic and found to be tolerable and feasible. Evidence to date suggests that CD40 activation is a critical and nonredundant mechanism to convert so-called cold tumors to hot ones (with prominent tumor infiltration of T cells), sensitizing them to checkpoint inhibition [25]. CXCR-4 is an alpha-chemokine receptor specific for stromal-derived-factor-1 (SDF-1, also known as CXCL12), which has been found to be expressed in more than 23 different types of cancers. The CXCR4/CXCL12 axis plays a relevant role in shaping the tumor microenvironment (TME), mainly towards dampening immune responses [26]. Previous suggests that the CXCR4-inhibiting nanocomplex decreases tumor fibrosis, facilitates T cell infiltration and relieves immunosuppression to modulate the immune process to improve the objective response rate of anti-PD-L1 immunotherapy [27]. As to TME, we all know that various cell types including B cell, T cell, tumor associated macrophages, dendritic cells, natural killer, myeloid-derived suppressor cells and signaling pathways within the TME can significantly influence tumor growth, spread, and metastasis, and they play a key role in determining tumor sensitivity to treatment. Given the complexity of TME, TME can be categorized into different types, as each type may respond differently to specific immunotherapies. In some report, TME can be divided into (infiltrated-excluded, I-E) TME which also called 'cold' tumor, (infiltrated-inflamed, I-I) TME which also called 'hot' tumor and (tertiary lymphoid structures, TLS) TME. Different subtype produce different immune response.

Classical cancer-related signaling pathways play important role in the therapy for ESCC. Recent study based on the whole genomic, epigenomic, transcriptomic, and proteomic data of 155 ESCCs showed that the classification of ESCCs can be divided into four subtypes: cell cycle pathway activation, NRF2 oncogenic activation, immune suppression (IS), and immune modulation (IM). IS and IM cases were highly immune infiltrated but differed in the type and distribution of immune cells. IM cases showed better response to immune checkpoint blockade therapy than other subtypes in a clinical trial [28]. Genomic analyses reveal that the NOTCH pathway is associated with the progression of ESCC. The results showed that although the cancer-associated genes TP53, PIK3CA, CDKN2A and their pathways showed no significant difference between stage I and stage III tumors, a prevalence of mutations in NOTCH1 and in the NOTCH pathway that indicate that they are involved in the preclinical and early stages of ESCC [29]. There are some limitations for the study. First, absence of in vivo data impaired the impact of findings. Second, limited sample size of included esophageal cell lines although all the cell lines are common for experiments. Third, no direct comparison of the results with patient data which impaired the clinical significance. We hope, in the future, to employ the functional mechanism of significant genes and to make the results more clinical translational significance.

In conclusion, we first report the genomic and mRNA data of common ESCC cell lines. The data provide reference information for selecting appropriate cell lines for experiments. Invasion genes were up-regulated in the KYSE-150 cell line. Compared with other cell lines, ECA-109 exhibited an immune status.

Supplementary Information

The online version contains supplementary material available at https://doi.org/10.1186/s12935-025-03686-1.

Supplementary Material 1
Supplementary Material 2
Supplementary Material 3
Supplementary Material 4
Supplementary Material 5
Supplementary Material 6

Acknowledgements
Thanks for the Central Laboratory of Fudan University Shanghai Cancer Center.

Author contributions
Chao Zhang collected and prepared the cell lines for sequencing. Chao Zhang supplied the supplementary tables and wrote the paper. Chenghao Li analyzed the data and supplied Figs. 1, 2, 3 and 4. Jian zhong Su provided the analysis methods and sequencing depth. Longlong Shao purchased and donated the cell lines. Jiaying Deng designed the project and revised the manuscript.

Funding
There is no funding for the study.

Data availability
No datasets were generated or analysed during the current study.

Declarations

Ethics approval and consent to participate
Human ethics are not involved in this study. Cancer cell lines were purchased and donated. And all these cell lines have been identified EK-Bioscience company.

Consent for publication
All the authors review the manuscript and agree to publish the study in the journal.

Competing interests
The authors declare no competing interests.

Received: 28 July 2024 / Accepted: 10 February 2025
Published online: 09 May 2025

References

1. Torre LA, Bray F, Siegel RL, Ferlay J, Lortet-Tieulent J, Jemal A. CA Cancer J Clin. 2015;65(2):87–108.
2. Yang H, Liu H, Chen Y, Zhu C, Fang W, Yu Z, Mao W, Xiang J, Han Y, Chen Z, Yang H, Wang J, Pang Q, Zheng X, Yang H, Li T, Zhang X, Li Q, Wang G, Chen B, Mao T, Kong M, Guo X, Lin T, Liu M, Fu J. JAMA Surg. 2021;156(8):721–9.
3. Eyck BM, van Lanschot J, Hulshof M, van der Wilk BJ, Shapiro J, van Hagen P, van Berge HM, Wijnhoven B, van Laarhoven H, Nieuwenhuijzen G, Hospers G, Bonenkamp JJ, Cuesta MA, Blaisse R, Busch OR, Creemers GM, Punt C, Plukker J, Verheul H, Spillenaar BE, van der Sangen M, Rozema T, Ten KF, Beukema JC, Piet A, van Rij CM, Reinders JG, Tilanus HW, Steyerberg EW, van der Gaast A. J Clin Oncol. 2021;39(18):1995–2004.
4. Lin DC, Hao JJ, Nagata Y, Xu L, Shang L, Meng X, Sato Y, Okuno Y, Varela AM, Ding LW, Garg M, Liu LZ, Yang H, Yin D, Shi ZZ, Jiang YY, Gu WY, Gong T, Zhang Y, Xu X, Kalid O, Shacham S, Ogawa S, Wang MR, Koeffler HP. Nat Genet. 2014;46(5):467–73.
5. Song Y, Li L, Ou Y, Gao Z, Li E, Li X, Zhang W, Wang J, Xu L, Zhou Y, Ma X, Liu L, Zhao Z, Huang X, Fan J, Dong L, Chen G, Ma L, Yang J, Chen L, He M, Li M, Zhuang X, Huang K, Qiu K, Yin G, Guo G, Feng Q, Chen P, Wu Z, Wu J, Ma L, Zhao J, Luo L, Fu M, Xu B, Chen B, Li Y, Tong T, Wang M, Liu Z, Lin D, Zhang X, Yang H, Wang J, Zhan. Q Nat. 2014;509(7498):91–5.
6. Deng J, Chen H, Zhou D, Zhang J, Chen Y, Liu Q, Ai D, Zhu H, Chu L, Ren W, Zhang X, Xia Y, Sun M, Zhang H, Li J, Peng X, Li L, Han L, Lin H, Cai X, Xiang J, Chen S, Sun Y, Zhang Y, Zhang J, Chen H, Zhang S, Zhao Y, Liu Y, Liang H, Zhao K. Nat Commun. 2017;8(1):1533.
7. Cui Y, Chen H, Xi R, Cui H, Zhao Y, Xu E, Yan T, Lu X, Huang F, Kong P, Li Y, Zhu X, Wang J, Zhu W, Wang J, Ma Y, Zhou Y, Guo S, Zhang L, Liu Y, Wang B, Xi Y, Sun R, Yu X, Zhai Y, Wang F, Yang J, Yang B, Cheng C, Liu J, Song B, Li H, Wang Y, Zhang Y, Cheng X, Zhan Q, Li Y, Liu Z. Cell Res. 2020;30(10):902–13.
8. Kato K, Shah MA, Enzinger P, Bennouna J, Shen L, Adenis A, Sun JM, Cho BC, Ozguroglu M, Kojima T, Kostorov V, Hierro C, Zhu Y, McLean LA, Shah S, Doi T. Future Oncol. 2019;15(10):1057–66.
9. Kojima T, Shah MA, Muro K, Francois E, Adenis A, Hsu CH, Doi T, Moriwaki T, Kim SB, Lee SH, Bennouna J, Kato K, Shen L, Enzinger P, Qin SK, Ferreira P, Chen J, Girotto G, de la Fouchardiere C, Senellart H, Al-Rajabi R, Lordick F, Wang R, Suryawanshi S, Bhagia P, Kang SP, Metges JP. J Clin Oncol. 2020;38(35):4138–48.
10. Okawa Y, Sasagawa S, Kato H, Johnson TA, Nagaoka K, Kobayashi Y, Hayashi A, Shibayama T, Maejima K, Tanaka H, Miyano S, Shibahara J, Nishizuka S, Hirano S, Seto Y, Iwaya T, Kakimi K, Yasuda T, Nakagawa H. Cancer Lett. 2024;581:216499.
11. Li H, Durbin R. Bioinformatics. 2010;26(5):589–95.
12. McKenna A, Hanna M, Banks E, Sivachenko A, Cibulskis K, Kernytsky A, Garimella K, Altshuler D, Gabriel S, Daly M, DePristo MA. Genome Res. 2010;20(9):1297–303.
13. Miller CT, Lin L, Casper AM, Lim J, Thomas DG, Orringer MB, Chang AC, Chambers AF, Giordano TJ, Glover TW, Beer DG, Oncogene. 2006;25(3):409–18.
14. Akaishi T. Nihon Geka Gakkai Zasshi. 1984;85(11):1440–53.
15. Ludwig ML, Kulkarni A, Birkeland AC, Michmerhuizen NL, Foltin SK, Mann JE, Hoesli RC, Devenport SN, Jewell BM, Shuman AG, Spector ME, Carey TE, Jiang H, Brenner JC. Oral Oncol. 2018;87:144–51.
16. Mann JE, Kulkarni A, Birkeland AC, Kafelghazal J, Eisenberg J, Jewell BM, Ludwig ML, Spector ME, Jiang H, Carey TE, Brenner JC. Head Neck. 2019;41(9):3114–24.
17. Vikova V, Jourdan M, Robert N, Requirand G, Boireau S, Bruyer A, Vincent L, Cartron G, Klein B, Elemento O, Kassambara A, Moreaux. J Theranostics. 2019;9(2):540–53.
18. Kawasaki Y, Okumura H, Uchikado Y, Kita Y, Sasaki K, Owaki T, Ishigami S, Natsugoe S. Ann Surg Oncol. 2014;21(7):2347–52.
19. Wang Q, Ma J, Lu Y, Zhang S, Huang J, Chen J, Bei JX, Yang K, Wu G, Huang K, Chen J, Xu S. Oncogene. 2017;36(37):5321–30.
20. Afjei R, Sadeghipour N, Kumar SU, Pandrala M, Kumar V, Malhotra SV, Massoud TF, Paulmurugan R. Cancers (Basel) 2022;14(24).
21. Lee JH, Rangappa S, Mohan CD, Sethi G, Lin ZX, Rangappa KS, Ahn KS, Biomolecules. 2019;9(10).
22. Taufani IP, Situmorang JH, Febriansah R, Tasminatun S, Sunarno S, Yang LY, Chiang YT, Huang CY. Hum Exp Toxicol. 2023;42:774799393.
23. Sunpaweravong P, Sunpaweravong S, Puttawibul P, Mitarnun W, Zeng C, Baron AE, Franklin W, Said S, Varella-Garcia M. J Cancer Res Clin Oncol. 2005;131(2):111–9.
24. Krykbaeva I, Bridges K, Damsky W, Pizzurro GA, Alexander AF, McGeary MK, Park K, Muthusamy V, Eyles J, Luheshi N, Turner N, Weiss SA, Olino K, Kaech SM, Kluger HM, Miller-Jensen K, Bosenberg M. Cancer Immunol Res. 2023;11(10):1332–50.
25. Vonderheide RH. Annu Rev Med. 2020;71:47–58.
26. Mezzapelle R, Leo M, Caprioglio F, Colley LS, Lamarca A, Sabatino L, Colantuoni V, Crippa MP, Bianchi ME. Cancers (Basel) 2022;14(9).
27. Li Z, Wang Y, Shen Y, Qian C, Oupicky D, Sun M. Sci Adv. 2020;6(20):eaaz9240.
28. Liu Z, Zhao Y, Kong P, Liu Y, Huang J, Xu E, Wei W, Li G, Cheng X, Xue L, Li Y, Chen H, Wei S, Sun R, Cui H, Meng Y, Liu M, Li Y, Feng R, Yu X, Zhu R, Wu Y, Li L, Yang B, Ma Y, Wang J, Zhu W, Deng D, Xi Y, Wang F, Li H, Guo S, Zhuang X, Wang X, Jiao Y, Cui Y, Zhan Q. Cancer Cell. 2023;41(1):181–95.
29. Cheng C, Cui H, Zhang L, Jia Z, Song B, Wang F, Li Y, Liu J, Kong P, Shi R, Bi Y, Yang B, Wang J, Zhao Z, Zhang Y, Hu X, Yang J, He C, Zhao Z, Wang J, Xi Y, Xu E, Li G, Guo S, Chen Y, Yang X, Chen X, Liang J, Guo J, Cheng X, Wang C, Zhan Q, Cui Y. Gigascience. 2016;5:1.

Publisher's note